Structural and mutational characterization of the catalytic A-module of the mannuronan C-5-epimerase AlgE4 from Azotobacter vinelandii

Rozeboom, Henriette J.; Bjerkan, Tonje M.; Kalk, Kor H.; Ertesvag, Helga; Holtan, Synnove; Aachmann, Finn L.; Valla, Svein; Dijkstra, Bauke W.; Ertesvåg, Helga; Holtan, Synnøve

Published in:
The Journal of Biological Chemistry

DOI:
10.1074/jbc.M804119200

Publication date:
2008

THE JOURNAL OF BIOLOGICAL CHEMISTRY VOL. 283, NO. 35, pp. 23819–23828, August 29, 2008

Structural and Mutational Characterization of the Catalytic A-module of the Mannuronan C-5-epimerase AlgE4 from *Azotobacter vinelandii*[*]

Received for publication, May 29, 2008 Published, JBC Papers in Press, June 23, 2008, DOI 10.1074/jbc.M804119200

Henriëtte J. Rozeboom[‡1], Tonje M. Bjerkan[§1,2], Kor H. Kalk[‡], Helga Ertesvåg[§], Synnøve Holtan[§], Finn L. Aachmann[§], Svein Valla[§3], and Bauke W. Dijkstra[‡4]

From the [‡]Laboratory of Biophysical Chemistry, GBB, University of Groningen, Nijenborgh 4, 9747 AG Groningen, The Netherlands and the [§]Department of Biotechnology, The Norwegian University of Science and Technology, Sem Sælands vei 6/8, N-7491 Trondheim, Norway

Alginate is a family of linear copolymers of (1→4)-linked β-D-mannuronic acid and its C-5 epimer α-L-guluronic acid. The polymer is first produced as polymannuronic acid and the guluronic acid residues are then introduced at the polymer level by mannuronan C-5-epimerases. The structure of the catalytic A-module of the *Azotobacter vinelandii* mannuronan C-5-epimerase AlgE4 has been determined by x-ray crystallography at 2.1-Å resolution. AlgE4A folds into a right-handed parallel β-helix structure originally found in pectate lyase C and subsequently in several polysaccharide lyases and hydrolases. The β-helix is composed of four parallel β-sheets, comprising 12 complete turns, and has an amphipathic α-helix near the N terminus. The catalytic site is positioned in a positively charged cleft formed by loops extending from the surface encompassing Asp[152], an amino acid previously shown to be important for the reaction. Site-directed mutagenesis further implicates Tyr[149], His[154], and Asp[178] as being essential for activity. Tyr[149] probably acts as the proton acceptor, whereas His[154] is the proton donor in the epimerization reaction.

Alginate is a family of linear copolymers of (1→4)-linked β-D-mannuronic acid (M)[5] and its C-5 epimer α-L-guluronic acid (G) produced by brown algae and some bacteria belonging to the *Pseudomonas* and *Azotobacter* genera (1–4). The M- and G-moieties are distributed irregularly as blocks of homopolymeric regions (M- or G-blocks) interspersed with blocks of alternating structure (MG-blocks). The relative amounts and sequence distributions of M and G vary considerably between alginates from different sources, and this variation in sequence and composition imparts different properties to alginates. G-blocks are rather stiff, and form strong, brittle gels with divalent cations such as Ca^{2+}, whereas M-blocks are less rigid and do not form cationic gels. MG-blocks are the most flexible and have been shown to bind Ca^{2+} and form junction zones (5).

In *Azotobacter vinelandii*, alginate constitutes a major part of the coat surrounding cells differentiated into resting stage cysts (6, 7), and alginate negative strains do not encyst (8). Nevertheless, the polymer is also produced during vegetative growth, and under such conditions it may play a role in protecting the bacterium from oxidative stress (9).

The alginate polymer is produced as polymannuronic acid, and the guluronic acid residues are introduced at the polymer level by the action of mannuronan C-5-epimerases (10). All known alginate-producing bacteria possess a periplasmic C-5-epimerase, AlgG (11), but *A. vinelandii* also secretes a family of seven extracellular, Ca^{2+}-dependent mannuronan C-5-epimerases, *algE1–7* (12, 13). These enzymes are highly homologous and consist of one or two catalytic A-modules and one to seven regulatory R-modules, of which at least one is needed for full activity (14). Each of the extracellular *A. vinelandii* enzymes produces a distinctive M/G-pattern (14); AlgE2 and AlgE5 make relatively short G-blocks, whereas AlgE6 makes longer G-blocks (13, 15). AlgE4 almost exclusively produces alternating MG sequences (16).

AlgE4 is the smallest of the extracellular epimerases with a molecular mass of 57.7 kDa (553 amino acids). It contains one A-module, which is active on its own, comprising the 385 N-terminal amino acids, and one R-module of 142 residues, connected by a 7-residue linker. At the C terminus it has a small "S motif" of 19 residues of unknown function (12). Atomic force microscopy studies have revealed that the AlgE4 A-module binds more strongly to the alginate chain than the complete enzyme, indicating that the R-module is involved in the regulation of the enzyme-substrate binding strength (17). Nevertheless, the R-module on its own is also able to bind to the alginate chain (18).

AlgE4 has its optimum activity around pH 6.5–7.0 in the presence of 1–3 mM Ca^{2+} and at temperatures close to 37 °C (16). It is highly sensitive to alkaline pH, being inactive at pH > 8. It binds a minimum of 6 sugar residues in the catalytic site,

* This work was supported by a grant from the Norwegian Research Council. The costs of publication of this article were defrayed in part by the payment of page charges. This article must therefore be hereby marked "*advertisement*" in accordance with 18 U.S.C. Section 1734 solely to indicate this fact.

The atomic coordinates and structure factors (codes 2PYG and 2PYH) have been deposited in the Protein Data Bank, Research Collaboratory for Structural Bioinformatics, Rutgers University, New Brunswick, NJ (http://www.rcsb.org/).

[1] Both authors contributed equally to the article.

[2] Present address: SINTEF Materials and Chemistry, Biotechnology, N-7465 Trondheim, Norway.

[3] To whom correspondence may be addressed. E-mail: svein.valla@biotech.ntnu.no.

[4] To whom correspondence may be addressed. E-mail: b.w.dijkstra@rug.nl.

[5] The abbreviations used are: M, β-D-mannuronic acid; MG-blocks, stretches of contiguous alternating structure ($(MG)_n$); G, α-L-guluronic acid; G-blocks, stretches of contiguous G-residues; EMP, ethyl-mercury-phosphate; PL, polysaccharide lyase; MOPS, 3-(*N*-morpholino)propanesulfonic acid.

and for short chains the third residue from the non-reducing end is the first to be epimerized (19). For longer chains the reaction proceeds toward the reducing end in a non-random, processive manner (20). On average, the enzyme epimerizes 10 units ($(MG)_{10}$) in each reaction before leaving the chain (19).

An alignment of all known mannuronan C-5-epimerase sequences from bacteria and algae showed that they share an YG(F/I)DPH(D/E) motif (residues 149–155 in AlgE4) (21–23). Asp^{152} of this motif, which is also conserved in some pectate lyases, has been shown to be important for activity in AlgE7 (21). The reaction mechanism of C-5-epimerases has been proposed to be similar to the lyase reaction (24), involving three steps. First, the target uronic acid charge is neutralized, after which the proton at C-5 is abstracted. An enolate anion intermediate is formed, which is stabilized by resonance. In the lyase case, the enolate anion leads to β-elimination of the 4-*O*-glycosidic bond, whereas in the epimerase case β-elimination is prevented by donation of a proton to the opposite face of the sugar ring. Indeed in the bifunctional epimerase/lyase AlgE7 mutation of Asp^{152} eliminated both activities, suggesting that they occur at the same site (21). Here we report the three-dimensional structure of the AlgE4 A-module, which is responsible for generating MG-alginates, and discuss the location of the active site and a possible catalytic mechanism.

EXPERIMENTAL PROCEDURES

Growth of Bacteria—The bacterial strains and plasmids used in this study are listed in Table 1. Unless stated otherwise, bacteria were maintained at 37 °C in L broth (10 g of tryptone, 5 g of yeast extract, and 5 g of NaCl per liter) or on L agar (L broth supplemented with 15 g of agar per liter). Protein was expressed in 3× L broth (30 g of tryptone, 15 g of yeast extract, and 5 g of NaCl per liter). Media were supplemented with 200 μg/ml ampicillin or 12.5 μg/ml tetracycline when appropriate.

Recombinant DNA Technology—Standard recombinant DNA procedures were done according to Sambrook and Russell (25), whereas transformations were carried out according to the RbCl transformation protocol (New England BioLabs). Plasmids were isolated using the Wizard® *Plus* SV minipreps DNA Purification System (Promega). All gene manipulations were done in *Escherichia coli* DH5α, and the pTB26 plasmid was later transferred to *E. coli* ER2566 (New England BioLabs). DNA sequencing was performed using the BigDye® Terminator version 1.1 Cycle Sequencing Kit (Applied Biosystems).

Production and Purification of Mannuronan Oligomers—Partial acid hydrolysis of mannuronan was performed essentially as described by Campa *et al.* (19). Briefly, after pre-hydrolysis at pH 5.6, the sample was incubated for 6 h at 95 °C and pH 3.5, and then neutralized with NaOH. The resulting oligomannuronic acid hydrolysis mixture was fractionated on three serially connected columns of Superdex 30 preparative grade (HiLoad 2.6 × 60 cm, GE Healthcare) at a flow rate of 0.8 ml/min with 0.1 M NH_4Ac (pH 6.9) at room temperature. Fractions of 5 ml were collected from three successive column runs and pooled. The pooled samples were stored at 4 °C prior to three cycles of freeze-drying to remove all traces of NH_4Ac and to provide solid, purified oligomers of mannuronic acid.

Protein Expression and Purification—The A-module of AlgE4 was recombinantly expressed from pTB26, a derivative of the IMPACT-CN expression vector pTYB4 (New England BioLabs) with the sequence encoding the first 378 amino acids of AlgE4 inserted (Table 1). AlgE4A was expressed in *E. coli* ER2566 at 15 °C and purified in a single affinity chromatography step, using the IMPACT-CN Protein Fusion and Purification System (New England BioLabs), as described in the manual.

Secondary Structure Determination—Circular dichroism studies of AlgE4A were carried out with a protein concentration of 5 μM in 100 μM HEPES (pH 6.9), at 293 K, and 5 mM $CaCl_2$ on a JASCO J-175 spectropolarimeter. The resulting spectrum was the average of 12 scans recorded at a rate of 50 nm/min; it was analyzed by the program K2d (26).

Crystallization—Crystallization conditions were difficult to find; over 500 different conditions were tested before the first protein crystals appeared. AlgE4A crystals were obtained after two months from hanging drop experiments with 1.6–1.7 M sodium malonate (pH 7–8) as precipitant at room temperature, using drops of 3 μl of protein (11 mg/ml) and 3 μl of reservoir solution (27). The lozenge-shaped crystals had a typical size of $0.3 \times 0.2 \times 0.1$ mm^3.

X-ray Data Collection—Before data collection, crystals were soaked for 1 min in a cryoprotectant solution containing 1.7 M malonate and 20% glycerol, directly followed by flash cooling. Data were collected in house at 100 K on a DIP2030H image plate detector (Bruker-AXS, Delft, The Netherlands) using Cu-Kα radiation from a Bruker-AXS FR591 rotating-anode generator equipped with Franks mirrors. Intensity data were processed using DENZO and SCALEPACK (28). A highly redundant native data set to 2.1-Å resolution was obtained. The crystals belong to space group $P2_12_12$ (Table 2). With two monomers of 39.8 kDa in the asymmetric unit, the V_M is 3.0 $Å^3$/Da (29), and the calculated solvent content is 59%. Preparation of heavy atom derivatives was done by conventional soaking experiments (30) with 1–5 mM of the heavy atom compound. For substrate binding studies crystals were soaked for 18 h in a saturated solution of M_4 (an oligomer of four (1→4)-linked β-D-mannuronic acid residues) in 50% (*w/v*) polyethylene glycol 3350, and 10 mM $CaCl_2$ at pH 6.5. The M_4 dataset was collected at Bruker-AXS, Delft, using Cu-Kα radiation from a Bruker-AXS Microstar generator with Montel200 multilayer graded optics, and a Proteum-R diffractometer system with a 3-axis goniostat, at a temperature of 100 K.

Structure Determination—The structure of AlgE4A was determined by multiple isomorphous replacement with two heavy atom derivatives (Table 2). Heavy atom positions were located with the program SOLVE (31), which was also used for refining the heavy atom parameters and for calculating phases. Density modification and phase extension to 2.1 Å was done with RESOLVE (31), which was also used to automatically build fragments of the main chain. After RESOLVE, the overall figure of merit was 0.45. At this stage, a 2.1-Å electron density map was calculated and visually inspected with the program O (32). The map was judged not to be interpretable; no electron density was visible for residues that had not been built by RESOLVE. Moreover, the direction of the main chain could not be deduced

TABLE 1
Bacterial strains and plasmids

Strains or plasmids	Relevant characteristics[a]	Mutagenic oligonucleotide[b]	Refs.
E. coli			
DH5α			25
ER2566	Encodes T7 RNA polymerase		New England Biolabs
Plasmids			
pTYB4	IMPACT-CN fusion vector containing a C-terminal chitin binding Tag		New England BioLabs
pUC7Tc	pUC7 containing the *tetAR* genes from RK2, Ap^r, Tc^r		53
pBL5	Derivative of pTrc99A encoding *algE4* from *A. vinelandii*, Ap^r		51
pTB22	Derivative of pTYB4 in which a NcoI-XmaI fragment of pBL5 containing *algE4* was inserted into the corresponding sites of the vector		This study
pTB26	Derivative of pTB22 in which the *tetAR* genes from a pUC7Tc BamHI-fragment was blunt-end ligated into the unique Eco47III site of the vector Tc^r		This study
pTB61	*algE4* H154F (removing BssSI)	CGGCTTCGACCCCttCGAGCAGACC	This study
pTB62	*algE4* Y149F (inserting BspEI)	CGAGATGTCCGGaTtCGGCTTC	This study
pTB63	*algE4* Y149H (inserting BspEI)	CGAGATGTCCGGacACGGCTTC	This study
pTB64	*algE4* K117E (removing SalI)	ACCAGCGGCgAaGTtGACGGCTGGT	This study
pTB65	*algE4* K117R (inserting NotI)	AACACCAGCGGCcgcGTCGACGGCTGGTTC	This study
pTB67	*algE4* F122Y (inserting RsaI)	CGACGGCTGGTaCAACGGCTATATC	This study
pTB69	*algE4* D173V (removing BglI)	CAACGGCCTCGtgGGaTTCGTCGCCGAC	This study
pTB70	*algE4* R195L (inserting BspMI)	GCCAACGACCtgCACGGCTTCAAC	This study
pTB71	*algE4* D152E (inserting BstBI)	ACGGCTTCGAaCCCCACGAG	This study
pTB72	*algE4* D152N (removing BssSI)	CTACGGCTTCaACCCCCAtGAGCAGACC	This study
pTB73	*algE4* H154Y (removing BssSI)	CTTCGACCCCtACGAGCAGACC	This study
pTB74	*algE4* R195K (removing BtgI)	CGCCAACGACaagCACGGCTTC	This study
pTB75	*algE4* D173N (inserting BsaI)	GACAACGGtCTCaACGGCTTCGTC	This study
pTB76	*algE4* D173E (inserting XhoI)	CAACGGCCTCGAgGGCTTC	This study
pTB78	*algE4* P153A (inserting BspHI)	CGGCTTCGACgCtCAtGAGCAGACC	This study
pTB79	*algE4* R249A (inserting Eco57I)	GACAACGCCgctGAAGGCGTGCTG	This study
pTB80	*algE4* F122V (inserting HpaI)	CGACGGCTGGgTtAACGGCTATATC	This study
pTB82	*algE4* D178E (removing SexAI)	CGGCTTCGTCGCCGAaTAtCTGGTC	This study
pTB83	*algE4* D178N (inserting NruI)	GACGGCTTCGTCGCgaAtTACCTG	This study
pTB84	*algE4* Q225E (removing BsgI, inserting BsrBI)	CCTGGTGGTGgAGCGGGGTCTG	This study
pTB87	*algE4* D152N, D173E; derivative of pTB72 (inserting XhoI)	CAACGGCCTCGAgGGCTTC	This study
pTB89	*algE4* D173E, P153A; derivative of pTB76 (inserting BspHI)	CGGCTTCGACgCtCAtGAGCAGACC	This study
pTB92	*algE4* Q225N (removing BsgI)	CCTGGTGGTGaAtCGGGGTCTGG	This study
pTB93	*algE4* K255R (inserting BspEI)	GTGCTGCTCcgGATGACCAGCGACATCAC	This study
pTB147	*algE4* E155A (removing BssSI)	GACCCCCACGcGCAGACCATCAACC	This study
pTB153	*algE4* Y149A (inserting NgoMIV)	CGAGATGTCCGGCgcCGGCTTCGACCC	This study
pTB154	*algE4* D152A (inserting BseRI)	GGCTACGGCTTCGctCCtCACGAGCAGACC	This study
pTB155	*algE4* H154A (removing BssSI, inserting PvuII)	GGCTACGGCTTCGACCCagctGAGCAGACCATC	This study
pTB156	*algE4* D173A (inserting NaeI)	CAACGGCCTCGcCGGCTTCGTCGC	This study
pTB157	*algE4* D178A (removing SexAI)	CTTCGTCGCCGcaTAtCTGGTCGACAG	This study
pTB158	*algE4* D173V, R195L; derivative of pTB69 (inserting BspMI)	GCCAACGACCtgCACGGCTTCAAC	This study
pHE186	*algE4* H154R (removing BssSI)	GCTTCGACCCaCgCGAGCAGACCATCAAC	This study
pHE187	*algE4* H154K (removing BssSI)	CGGCTTCGACCCtaAgGAGCAGACCATC	This study
pTB185	*algE4* H196A (inserting NaeI)	CTACGCCAACGACCGCgcCGGCTTCAAC	This study
pTB186	*algE4* H196F (inserting PvuI)	CTACGCCAACGAtCGCttCGGCTTCAAC	This study
pTB187	*algE4* H196Y (inserting PvrI)	CTACGCCAACGAtCGCtACGGCTTCAAC	This study
pTB188	*algE4* K117A (removing SalI)	CAACACCAGCGGCgcGGTtGACGGCTGGTTC	This study
pTB190	*algE4* Q156A (removing BssSI)	CTTCGACCCCCACGAagcGACCATCAACCTG	This study
pTB191	*algE4* E155A, Q156A (removing BssSI)	CTTCGACCCCCACGcGgcGACCATCAACCTG	This study
pTB192	*algE4* Q225A, K255A; derivative of pTB193 (inserting NruI)	GAAGGCGTGCTGCTCgcGATGACCAGCG	This study
pTB193	*algE4* Q225A (inserting SmaI)	GCCTGGTGGTGgccCGGGGTCTGGAGG	This study
pTB194	*algE4* K255A (removing NruI)	GAAGGCGTGCTGCTCgcGATGACCAGCG	This study

[a] The abbreviations used are: Ap^r, ampicillin resistance; Tc^r, tetracycline resistance. Plasmids pTB61–194 and pHE186–187 are identical to pBL5 with the exception of the introduced mutation in *algE4*.
[b] These are the forward primers; the reverse primers were complementary to them. Changed bases are shown in lower case. In pTB87, pTB89, pTB158, and pTB192, pBL5 was not used as the template.

TABLE 2
Data collection and phasing statistics

Crystal/derivative	Native	EMP ($C_2H_5HgPO_4$)	$PtCl_4$	M_4
Cell (Å)	174.0, 121.3, 44.7	174.0, 121.2, 44.6	174.0, 121.3, 44.7	169.6, 121.8, 45.1
Resolution range (Å)	50.0–2.1 (2.18–2.1)	50.0–2.8 (2.9–2.8)	50.0–3.2 (3.31–3.2)	43.6–2.7
No. of unique reflections	51,691 (4,598)	19,544 (1,886)	14,451 (1,368)	26,719
Completeness (%)	92.3 (83.6)	81.2 (80.7)	88.5 (87.4)	99.2 (93.8)
Overall $I/\sigma(I)$	12.4 (1.8)	11.6 (3.5)	11.8 (5.3)	10.7 (1.9)
R_{sym} (%)	9.8 (63.8)	9.6 (30.6)	13.0 (29.7)	10.0 (56.1)
No. of sites		2	1	-

and no side chain density was visible. Therefore, in an iterative procedure, phases were improved with the ARP/wARP procedure (33) combined with model building by hand. When 55% of the main chain had been built in this way, the phases could not be further improved. By assuming that the two heavy atoms from the EMP derivative occupy the same positions in the pro-

TABLE 3
Refinement statistics

	Native	M_4
Resolution (Å)	50.0-2.1	43.6-2.7
No. of reflections in working set	48,999	25,216
No. of reflections in test set	2,624	1,336
R_{work} (%)	19.4	23.3
R_{free} (%)	23.5	27.9
Root mean square deviations from ideal		
Bond length (Å)	0.006	0.007
Bond angles (deg)	1.29	1.30
Ramachandran plot		
Non-glycine residues in most favored regions (%)	84.3	
Non-glycine residues in additional allowed regions (%)	14.8	
Non-glycine residues in generously allowed regions (%)	1.0	
Number of non-hydrogen atoms (average *B* values (A)^2) total/main chain/side chain		
Residues in chain A	2–375	1–376
Protein molecule A	2,782 (33.5/33.0/34.0)	2,799 (49.8/49.6/50.0)
Residues in chain B	2–377	1–377
Protein molecule B	2,798 (31.0/32.5/31.7)	2,806 (47.5/47.2/47.8)
Water	520 (42.0)	61 (36.6)
Calcium ions	2 (33.8)	7 (72.5)
Glycerol	1 (60.6)	
Mannuronic acid		3 (107.0)

tein, and by overlaying parts of the already built main chain, the non-crystallographic symmetry operators could be determined. This allowed non-crystallographic symmetry averaging during refinement with CNS (34), and the gradual completion of the model building. The structure refinement converged at 2.1 Å to an R_{free} value of 23.5% and a conventional R_{factor} of 19.5%. The final model consists of 750 amino acids, residues 2–375 from molecule A and residues 2–377 from molecule B, 520 water molecules, 1 glycerol molecule, and 2 calcium ions. Assuming that the *B*-values of these calcium ions are similar to those of the neighboring protein atoms the occupancies of the calcium ions are close to 0.5 (Table 3). The stereochemistry of the final structure was evaluated using the program PROCHECK (35) (Table 3). For the M_4 experiment the native structure was used as the starting model. Initial $2F_o - F_c$ and $F_o - F_c$ maps clearly showed density for an M_3 trisaccharide product as well as for calcium and chloride ions. The atomic coordinates of the final models and structure factors have been deposited in the Protein Data Bank (entries 2PYG for the native structure and 2PYH for the M_4 structure).

Construction and Characterization of AlgE4 Mutants—Mutants of AlgE4 were constructed by the QuikChange™ Site-directed Mutagenesis Kit (Stratagene) according to the manufacturer's instructions using the primers shown in Table 1. AlgE4 mutant proteins (plasmids pTB61–pTB65; pTB67; pTB69–pTB76; pTB78–pTB80; pTB82–pTB84; pTB87; pTB89; pTB92–pTB93; pTB147; pTB153–pTB158; pTB185–pTB188; pTB190–pTB194; pHE186–pHE187) and the wild type AlgE4 (plasmid pBL5) were expressed in *E. coli* DH5α at 37 °C, partially purified by fast protein liquid chromatography on a HiTrap-Q column (GE Healthcare), and their catalytic activities measured in an isotope assay essentially as previously described (14), using two purification buffers and a disruption buffer containing 20 mM MOPS (pH 6.9) supplemented with 2 mM $CaCl_2$, 2 mM $CaCl_2$, 1 M NaCl, and 4 mM $CaCl_2$, respectively. Protein concentrations were estimated by the Bio-Rad protein assay (36).

RESULTS

Structure of the Mannuronan C-5-epimerase AlgE4 A-module—The crystal structure of the A-module of AlgE4 (AlgE4A) was determined at 2.1-Å resolution by the multiple isomorphous replacement method using two heavy atom derivatives (Table 2). There are two molecules, A and B, in the asymmetric unit. Residues 2–375 from molecule A and residues 2–377 from molecule B could be built into the electron density. Superimposition of the two molecules reveals that they are very similar with 373 Cα atoms overlaying with an root mean square deviation of only 0.20 Å.

The AlgE4A molecule folds into a right-handed parallel β-helix structure comprising 12 complete turns with overall dimensions of 67 × 37 × 36 Å (Fig. 1). The number of amino acid residues per turn varies from 20 to 40. The β-helix turns form four parallel β-sheets, named PB1, PB2a, PB2b, and PB3, consistent with the naming of the β-sheets in polygalacturonase II (37). Not being part of the β-helix, residues 307–309 and 316–318 make up a small two-stranded antiparallel β-sheet, whereas residues 19–32 form an amphipathic α-helix that caps the N-terminal end of the β-helix. The C-terminal end of the β-helix is covered by the C-terminal end of the second molecule in the asymmetric unit. This predominantly β-helical structure agrees with circular dichroism studies (Fig. 2), which suggest an α-helix content of 5%, a β-strand content of 47%, and a coil content of 48%, whereas, according to the DSSP algorithm (38), the crystal structure contains 3.5% α-helix, 46.5% β-strand, and 50% coiled coil.

Turns connect the β-strands in adjacent β-sheets. The T1 turns between PB1 and PB2 (a or b) vary in length from 1 to 19 amino acids, whereas the T2 turns between PB2 (a or b) and PB3 are short, consisting of one amino acid residue, except in the first three turns, which comprise 8, 2, and 7 residues, respectively. Between PB3 and PB1, the T3 turns vary from 4 to 12 amino acid residues. The T1 and T3 turns are longer toward the N- and C-terminal parts of the β-helix, respectively, and these extensions form a cleft across the

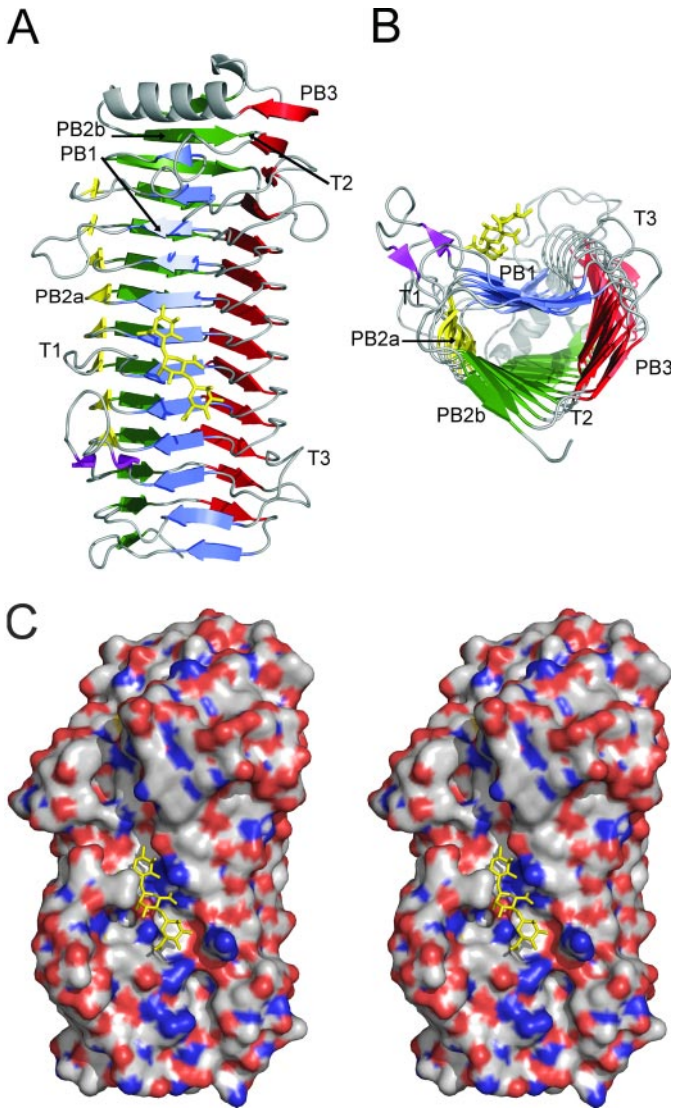

FIGURE 1. **Structure of AlgE4A.** A mannuronan trisaccharide (M_3) bound in the active cleft is shown in *stick* representation. *A*, the secondary structure elements forming the β-helix fold. The N-terminal α-helix is shown at the top. The 4 sheets forming the helix are colored *blue* (PB1), *yellow* (PB2a), *green* (PB2b), and *red* (PB3). The T1–T3 turns are also indicated. *B*, the same structure as in *A*, seen from the C-terminal end. *C*, stereo view of the electrostatic potential surface. Positive potential is shown in *blue* and negative potential in *red*. The figure was produced using PyMol (52).

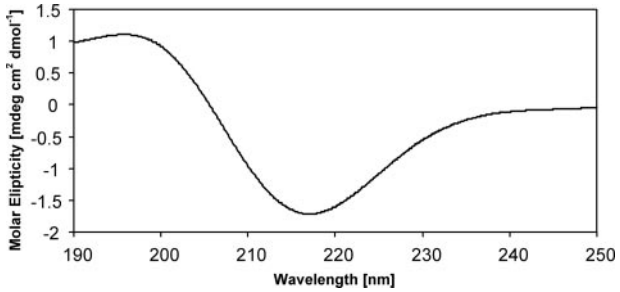

FIGURE 2. **Circular dichroism spectrum of 5 μM AlgE4A in 100 μM HEPES (pH 6.9), 20 °C, and 5 mM $CaCl_2$.** The spectrum of AlgE4A indicates high β-sheet structure content.

center of the molecule, of which the bottom is made up by PB1. In other β-helix proteins the active site is located in the cleft between the long T1 and T3 loops (37, 39), and also in AlgE4A the catalytically important residue Asp^{152} (21) is situated in this cleft.

A calcium ion with a pentagonal-bipyramidal coordination is bound in the hairpin loop between strands β7 and β8 (Fig. 3), with side chains of Ser^{91}, Thr^{97}, and Asp^{133} and the main chain carbonyl oxygen atoms of Glu^{95} and Gly^{124} coordinating the ion. No other calcium ions were present in the native structure, but after soaking crystals in 10 mM $CaCl_2$ five additional calcium binding sites were identified at the surface close to Glu^{376}–Ile^{357}, Glu^{229}, Thr^{114}–Arg^{111}, Asp^{112}–Glu^{145}–Asp^{169}, and Asp^{308}–Thr^{310}. In addition, a chloride ion is bound to Arg^{90} under these conditions. A glycerol molecule from the cryoprotectant is present in the active site in molecule A, close to His^{154}, Asp^{178}, and Tyr^{149}. Glycerol hydroxyl groups are known to often mimic binding of the oxygen atoms of a saccharide substrate (40). One *cis*-peptide is present between Glu^{155} and Gln^{156}. In proteins in which non-proline *cis*-peptide bonds have been identified, they often occur at or near functionally important sites and are likely involved in catalysis (41).

Location of the Active Site—To investigate the interaction of AlgE4A with substrate, crystals were soaked in a solution of M_4, a tetrasaccharide of four (1→4)-linked β-D-mannuronic acid residues. After overnight soaking electron density was only observed for a trisaccharide (M_3), bound in subsites −3, −2, and −1 (subsite nomenclature according to Ref. 42, the epimerization reaction takes place in subsite +1). The binding of the trisaccharide does not influence the overall structure of the enzyme; the room mean square deviation of all Cα atoms is only 0.27 Å between native and trisaccharide-bound AlgE4A. The bound trisaccharide adopts a linear conformation and has its non-reducing end in subsite −3 toward the C-terminal end of the protein (Fig. 3; see Table 4 for a summary of the hydrogen bonding interactions between the bound trisaccharide and AlgE4A). A shorter soaking time of 4 h revealed some extra electron density in the +1 subsite, close to Asp^{152}, a residue previously implicated in catalysis (21), suggesting that during the overnight soaking the substrate had degraded. However, density in the +1 subsite was not clear enough to allow reliable modeling of a tetrasaccharide.

To assess the importance of other amino acids for catalysis and binding of the alginate substrate, numerous mutants of AlgE4 were constructed (Fig. 4), based on its alignment with AlgE1–7 and their essentially inactive homologue AlgY (13). Four residues, Tyr^{149}, Asp^{152}, His^{154}, and Asp^{178}, all located in subsite +1, were found to be absolutely essential for AlgE4 activity. The first three of these amino acids are conserved in all known mannuronan C-5-epimerases, whereas Asp^{178} seems to be conserved in the *A. vinelandii* enzymes only. Tyr^{149}, His^{154}, and Asp^{178} point with their side chains into the +1 subsite (Fig. 3), and are likely to interact with a sugar bound at this subsite. Even conservative replacements of these three residues result in essentially inactive enzymes, strongly suggesting a role in catalysis. Replacement of Asp^{152} by a Glu makes the enzyme practically inactive and only 1% of the activity remains when it is replaced by an Asn (Fig. 4). Thus, both the charge and the size of this residue are important.

In the active site, Pro^{153} and the *cis*-peptide between Glu^{155} and Gln^{156} appear as important elements for providing an exact

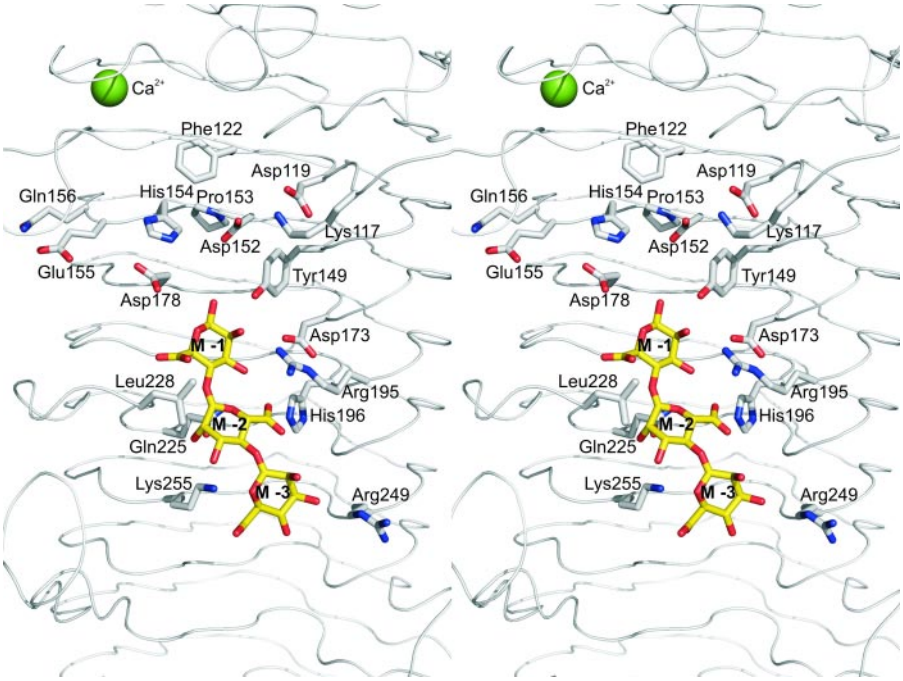

FIGURE 3. **Stereo view of amino acids surrounding the substrate binding site.** A bound mannuronan trisaccharide (M_3) molecule is shown in *stick* representation. Glu^{155} and Gln^{156} form a *cis*-peptide. The image was constructed in PyMOL (52).

TABLE 4
Interactions between bound sugar atoms and AlgE4A

Sugar atom	Protein atom	Distance
		Å
M-3 O-5	Lys^{255} NZ	3.7
M-3 O-6A	Lys^{255} NZ	4.0
M-3 O-6B	Lys^{255} NZ	3.2
M-2 O-2	Gln^{225} OE1	2.5
M-2 O-3	Lys^{255} NZ	3.8
M-2 O-5	Gln^{225} NE2	3.2
M-2 O-6A	Arg^{195} NH_2	3.5
	His^{196} NE2	2.9
	Gln^{225} NE2	3.7
M-2 O-6B	Arg^{195} NH1	4.0
M-1 O-1	Tyr^{149} OH	3.0
M-1 O-2	Tyr^{149} OH	2.5
M-1 O-3	Asn^{199} ND2	3.0
M-1 O-3	Arg^{195} NH_2	2.6
M-1 O-6B	Leu^{228} N	2.9

geometry around the catalytic site. Indeed replacement of Pro^{153} with Ala resulted in a 10-fold drop in activity. An even more dramatic effect was seen when replacing Glu^{155} with Ala, leading to a near 1000-fold drop in activity. This residue is unlikely to interact directly with the substrate but the substitution probably leads to the disruption of the *cis* peptide. In contrast, the replacement of Gln^{156} with Ala leads to a 10-fold activity drop, whereas replacements by other amino acids (results not shown) result in no detectable activity changes, implying that Gln^{156} is neither essential for the *cis* peptide nor for the catalysis, however, in combination with E155A, Q156A leads to an essentially inactive enzyme.

Residues Involved in Substrate Binding—Exchange of Arg^{195} with Lys reduced the activity of AlgE4 ~30-fold, whereas its replacement by Leu made the enzyme essentially inactive (0.2% activity) (Fig. 4). Arg^{195} binds the alginate chain in subsite −1 (Table 4). Its side chain orientation is stabilized by hydrogen bonding interactions with the carboxylate group of Asp^{173} (2.8 and 3.1 Å). The Asp^{173} side chain has additional hydrogen bonds with the peptide nitrogen atom of His^{196} (3.2 Å), and with the N-δ2 atom of Asn^{199} (3.0 Å). Substitution of Asp^{173} with the somewhat larger Glu apparently leaves these interactions mostly intact, because this mutant protein displays only a slight drop in activity, and has limited additive effect in combination with D152N or P153A. In contrast, the D173N mutant has lost most of its activity, presumably due to an impaired interaction with Arg^{195}. Thus Asp^{173} appears to be important for maintaining a productive conformation of Arg^{195} for substrate binding, consistent with the activity data for D173A, D173V, R195L, and the corresponding double mutant (Fig. 4). Indeed, the Asp^{173}–Arg^{195} pair is absolutely conserved in *A. vinelandii* AlgE1–7. Substitutions of His^{196} by Ala, or Tyr, reduced the AlgE4 activity 20–30-fold, whereas its replacement by Phe resulted in a 100-fold activity drop. The N-ϵ2 atom of His^{196} interacts with the M-6OA in subsite −2, implying an important role of His^{196} in substrate binding.

Gln^{225} interacts with the alginate chain in subsite −2. Exchange of this residue with Ala, Asn, or Glu reduced the activity about 10–20-fold, demonstrating its importance for substrate binding. The replacement of Lys^{255} by an Arg decreased the activity only slightly, but the activity decreased considerably when Lys^{255} was exchanged for an Ala. Lys^{255} is located near subsite −3 and may interact, either directly or via a water molecule, with the carboxylate of the mannuronic acid residue at subsite −3 (Table 4). The importance of these residues for substrate binding is also evident from the nearly total loss of activity for the double mutant Q225A, K255A. Mutants replacing Arg^{249} in subsite −4, on the other hand, keep most of the activity, implying that this residue is not important for substrate binding. Replacement of Lys^{117} in the proximity of subsites +1 and +2 into an Arg or Ala reduced the AlgE4 activity 4–6-fold. When it was changed to Glu (the amino acid found in AlgE7) the activity dropped to 3%. The positive charge is thus important at this site. Finally, Phe^{122} is located close to subsite +2 and probably interacts with the substrate in this site. Replacing Phe^{122} with Tyr resulted in only a minor drop in activity, whereas the replacement with Val led to a virtually inactive enzyme. The absence of structural data on the substrate binding mode in subsite +2 unfortunately precludes an explanation of these data.

DISCUSSION

AlgE4 is the first structurally characterized β-helix protein that catalyzes a C-5-epimerization reaction. Most β-helix proteins are hydrolases and lyases involved in the degradation of acidic

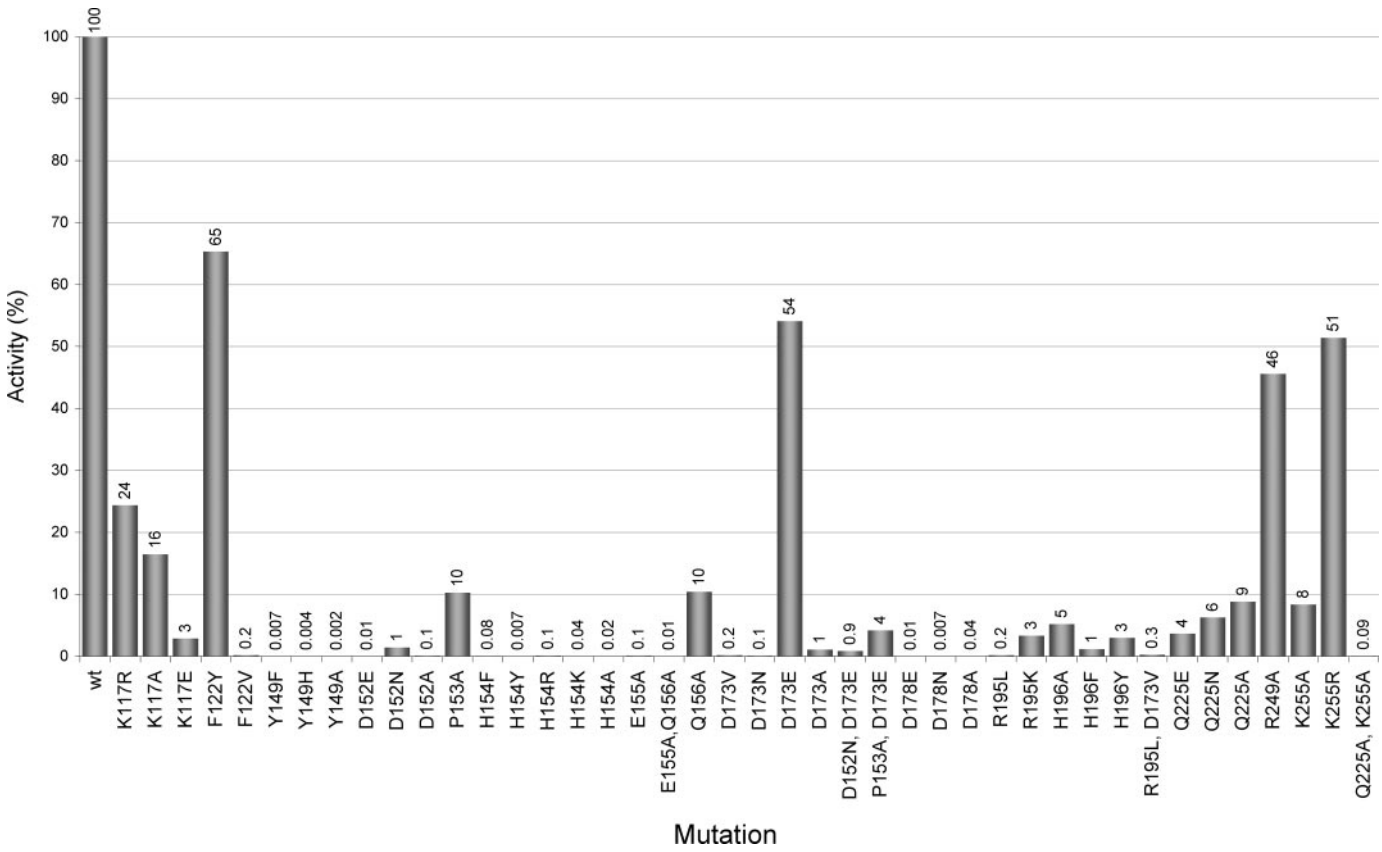

FIGURE 4. **Characterization of AlgE4 mutants.** Relative activities are shown compared with the wild type activity (100%). Enzymes showing less than 0.05% activity are considered inactive. Only enzymes with decreased activities to less than 60% are considered as being significantly different from the native enzyme.

polysaccharides. A Dali structural alignment search (43) revealed nine β-helix polysaccharide hydrolases and lyases with three-dimensional structures highly similar to AlgE4A (with Z-scores over 20). However, these proteins do not share any sequence homology that could suggest a common evolutionary origin, and their proposed catalytic residues are not conserved in AlgE4A.

In view of the proposed similarities in the catalytic mechanisms of alginate lyases and mannuronan C-5-epimerases, a comparison with the active sites of alginate lyases was made. So far, five alginate lyase crystal structures are available from 3 different polysaccharide lyase (PL) families (see Ref. 44). The alginate lyase A1-III from *Sphingomonas* species A1 (A1-III) is a PL-5 enzyme. Its structure (PDB 1HV6 (45)) is predominantly α-helical with a deep tunnel-like cleft, in which a mannuronic acid trimer can bind in an extended conformation (42). The other four crystal structures are the PL-7 alginate lyases PA1167 from *Pseudomonas aeruginosa* (PDB 1VAV (46)), ALY-1 from *Corynebacterium sp.* (PDB 1UAI (47)), A1-II′ from *Sphingomonas sp*. A1 (PDB 2CWS (48)), and a PL-18 alginate lyase from *Alteromonas sp*. 272 (PDB 1J1T). Although these enzymes consist, like AlgE4A, almost entirely of β-strands, their structures are quite different from that of AlgE4A. Instead of the parallel β-helix architecture of AlgE4 they display a jellyroll β-sandwich topology with antiparallel β-strands.

Osawa *et al.* (47) noted a striking agreement in spatial arrangement of four amino acid residues in the center of the substrate binding clefts of ALY-1 (PL-7) and A1-III (PL-5).

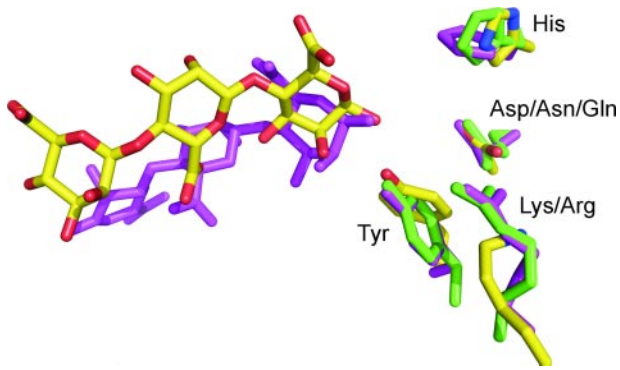

FIGURE 5. **Superimposition of the active site residues of ALY-1 in *green* (His^{119}, Gln^{117}, Arg^{72}, and Tyr^{195}), A1-III (His^{192}, Asn^{191}, Arg^{239}, Tyr^{246}, and trisaccharide) in *lilac*, and AlgE4A (His^{154}, Asp^{152}, Lys^{117}, and Tyr^{149} and trisaccharide) in CPK colors.** The image was constructed in PyMOL (52).

These residues were Gln/Asn, His, Arg, and Tyr. They were proposed to be the catalytic residues, with His functioning as the base in the reaction mechanism. The same spatial arrangement is also found in the other three lyases, and mutational studies of A1-II′ have indicated that the Tyr residue is particularly crucial for the catalytic reaction (48).

AlgE4A displays the same spatial arrangement of Asp^{152}, His^{154}, Lys^{117}, and Tyr^{149} in its active site (Fig. 5), and the mannuronic trisaccharide binds in a very similar orientation and position to that of the bound trisaccharide in A1-III. Although four active site amino acid residues seem to be positioned similarly, other important residues (particularly

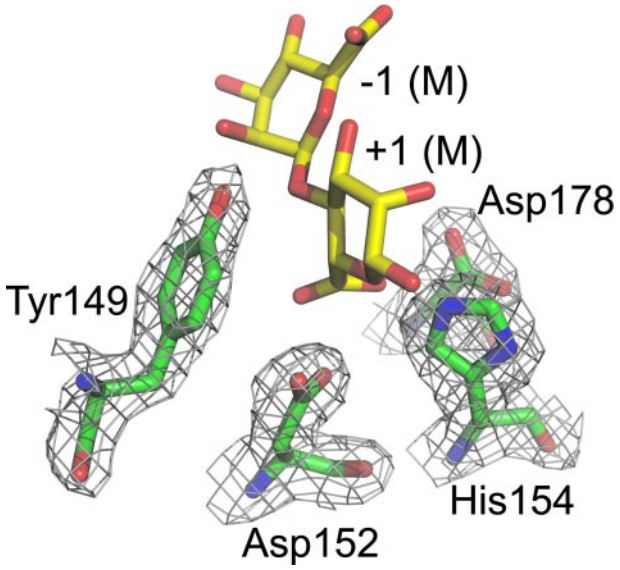

FIGURE 6. **$2F_o - F_c$ electron density of the native active site residues generated from a simulated-annealing composite omit map contoured at 1.5 σ.** The M residue in subsite −1 from the M_3 structure is superposed on the native structure, the M residue in the +1 site has been obtained by computer modeling. The figure was produced using PyMol (52).

Asp^{178}) and the environment at subsites −2 and −3 are very different.

The catalytic mechanism of mannuronan C-5-epimerases has previously been proposed to proceed in three steps: the abstraction of H-5, an inversion of the hexopyranose ring, and the donation of a proton to the opposite side of the pyranose ring (24). Tyr^{149}, Asp^{152}, His^{154}, and Asp^{178} are all positioned in the vicinity of the catalytic subsite (+1); moreover the replacement of these residues with other amino acids generally resulted in essentially inactive enzymes. To analyze the possible role of these residues in catalysis, a mannuronic acid residue in the $^4C_1$ chair conformation was modeled into subsite +1, by extending the experimentally observed bound M_3 trisaccharide chain with an extra M-unit (Fig. 6). The constraints imposed by the active site architecture resulted in only a limited number of possible positions for the +1 mannuronic acid residue without causing steric clashes. The allowed conformations are all very similar, and in all of them the +1 residue is oriented with its C-5 hydrogen atom pointing toward the Tyr^{149} hydroxyl group. Tyr^{149} is thus in a position fully compatible with a role as a general base (AA-2 in the model of Gacesa (24)), that abstracts the C-5-bound proton from the +1 M-residue. At the other face of the +1 sugar His^{154} is located, in an excellent position to act as a general acid (AA-3 (24)) that donates a proton to the C-5 atom of the +1 sugar, flipped into the $^1C_4$ chair conformation (Fig. 7).

The Tyr^{149} hydroxyl group is at hydrogen bonding distance to the Arg^{195} side chain (held in position by Asp^{173}), which provides a proton relay path to the solvent. This proposed role of Tyr^{149} resembles the proton abstraction step in chondroitin AC lyase, which also uses a tyrosine residue to abstract a proton, in this case from the C-5 atom of a glucuronic acid (49, 50). In addition, the reaction catalyzed by this latter enzyme proceeds via a similar putative enolic transition state as in the mannuronan C-5-epimerases and alginate lyases (42, 48). AlgE4 differs from the chondroitin AC lyase, though, in that the glycosidic bond between the −1 and +1 sugars remains intact, and Tyr^{149} does not donate its proton to the glycosidic oxygen. The essential role of His^{154} as a proton donor in M → G catalysis explains the lack of activity of AlgE4 at pH > 8 (16), at which pH the His^{154} side chain presumably is deprotonated.

An essential feature of the binding mode of the +1 mannuronic acid is that its carboxylic acid moiety points into the interior of the enzyme, and is at hydrogen bonding distance from the carboxylic acid side chains of Asp^{152} and Asp^{178}. It has been observed that for the activity of pectate/pectin lyases, which proceeds through a similar transition state as the mannuronan C-5 epimerases (24), an uncharged or methylated sugar carboxylate significantly enhances reactivity. The close interactions of the +1 carboxylic acid and the presumably negatively charged Asp^{152} (and/or Asp^{178}) side chain ensures that the sugar carboxylate will be protonated (AA-1 substrate stabilization (24)), and thus will be in an uncharged state promoting reactivity.

An intriguing question is how AlgE4 prevents the lyase side reaction. In principle, Tyr^{149} could donate the abstracted proton of the glycosidic oxygen of the bond between the −1 and +1 uronic acid residue, similar to, *e.g.* chondroitin AC lyase. We propose that the interaction between Tyr^{149} and Arg^{195} may provide an effective pathway to remove the proton from the active site, thus reducing the lyase activity. In addition, the hydrogen bonding interaction between the O-3 hydroxyl group of the +1 sugar and the ring O-5 atom of the −1 sugar residue may help to prevent the two sugars moving apart, which will also diminish the lyase reaction.

Although calcium is needed for the activity of AlgE4, no Ca^{2+} ion is found near the active site of the enzyme, neither in the native state nor after calcium soaking. However, the Ca^{2+} ion that was identified in the loop between strands β7 and β8 could very well explain the calcium dependence. In the absence of Ca^{2+} at this position, the loop would probably adopt a different conformation and the active site cleft could be disrupted.

Various positively charged protein side chains (Arg^{90}, Lys^{84}, Lys^{117}, Arg^{195}, His^{196}, and Lys^{255}) were identified that could stabilize the negative charge of the carboxylate side chains of the substrate. Of these residues, Arg^{195} and His^{196} bind the carboxylate side chain of the sugar residue at subsite −2, whereas Lys^{255} binds the one at subsite −3. Arg^{90} binds a chloride ion suggesting that it is also capable of binding the carboxylate side chain of a sugar residue. All these positively charged residues are positioned on one side of the active site cleft. The AlgE4-R-module also has a positively charged cleft on the surface of its β-helix (18). Connecting the C-terminal residue of the catalytic A-module to the N terminus of the R-module by a peptide bond would create one long β-helix protein, in which a continuous long substrate binding groove runs over the surface of the full-length AlgE4 epimerase (18), thus rationalizing the contribution of the R-module to substrate binding.

AlgE4 is a processive enzyme, which binds a minimum of six residues in the active site (19). The structure of the A-module shows that the polymer, which has to slide through the active site, is enclosed by two "clamps." The first clamp is between

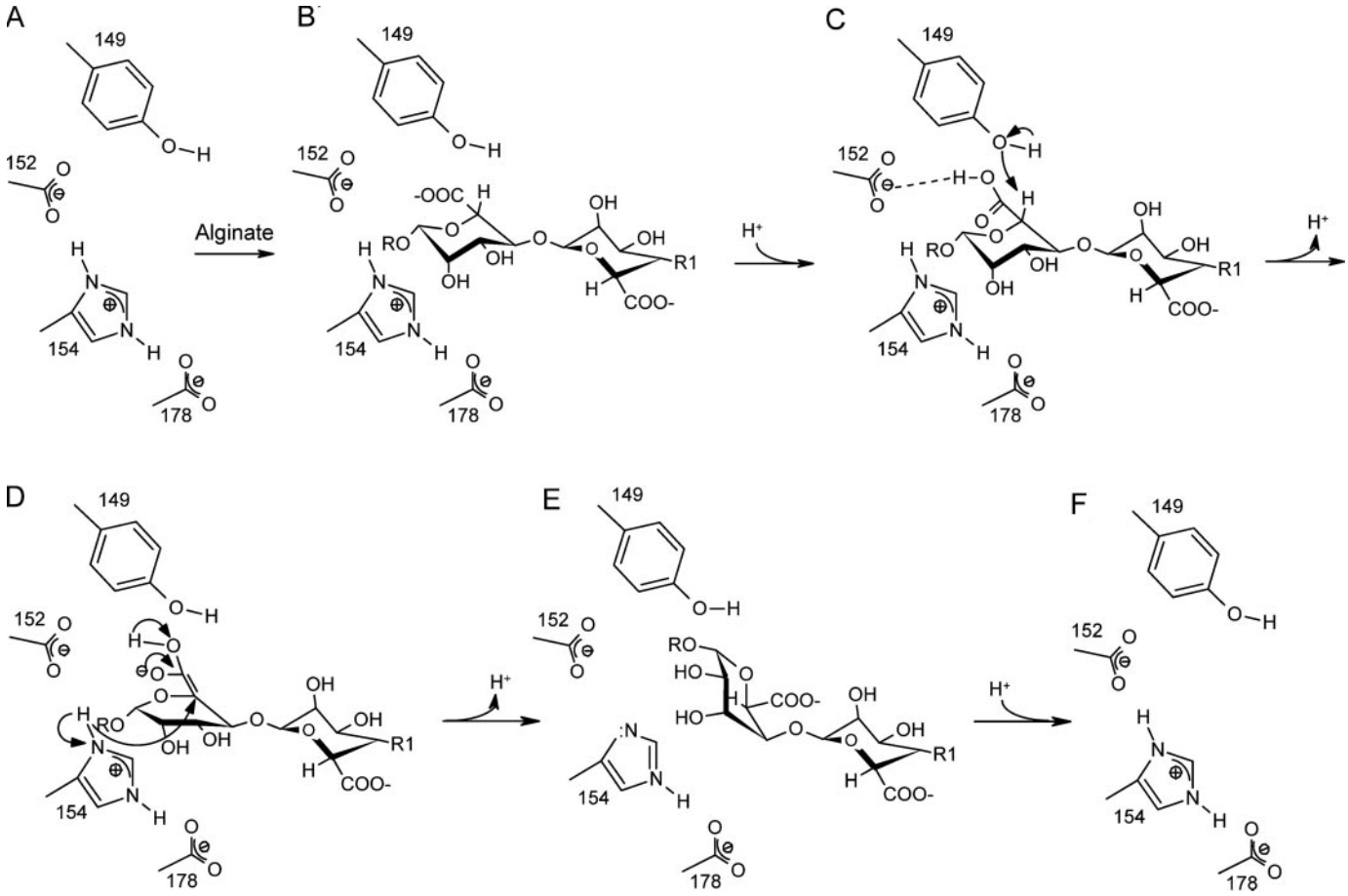

FIGURE 7. **Proposed catalytic mechanism of AlgE4.** *A* and *B*, the alginate polymer enters the catalytic site. *B* and *C*, the carboxylate moiety of the mannuronic acid in subsite +1 is protonated, enabling it to form a hydrogen bond with Asp[152] (and/or 178), which stabilizes the substrate-enzyme complex. *C*, upon deprotonation of Tyr[149] (via Arg[195]) the alkoxide ion group extracts H-5 from the *re*-face of the mannuronic acid in subsite +1. *C* and *D*, a double bond is formed, which makes the conformation of the +1 mannuronic acid partially planar. *D*, the protonated His[154] performs a nucleophilic attack on the C-5 atom of the +1 sugar from the *si*-face with the concomitant flip of the +1 sugar ring into the $^1C_4$ chair conformation of guluronic acid. *D* and *E*, the carboxylic acid moiety on sugar +1 is deprotonated. *E* and *F*, the epimerized sugar leaves the active site and His[154] is protonated again. *F*, the epimerase is ready to perform a new reaction.

Gly[53] and the Ca^{2+} binding loop with Tyr[93] at the tip, and Arg[90] at the bottom. The second clamp is between Arg[195] and a loop with Leu[228] at the tip, in the −2 subsite. These two clamps span a distance of about 20 Å, which can accommodate 5 sugar residues in a stretched conformation. The +1 site is at about 10 Å from either clamp. If the polymer chain has to slide through these positions it is also clear that, because of steric hindrance, O-2 and O-3 acetylated polymers cannot be epimerized, which explains why AlgE4A has no activity on such substrates. The importance of the second clamp is supported by hybrid enzyme studies in which residues 215 to 262 from AlgE4A, a processive enzyme, were transferred to AlgE2, a non-processive enzyme, converting it into a presumably processive enzyme (51).

It is still unclear how enzymes with the same catalytic residues distinguish between the formation of MG/GG-blocks and cleavage of the alginate chain. This reaction specificity must come from the environment of the active site, limiting which molecules effectively bind and also which reaction will take place. By comparing AlgE4 to the highly G-block forming enzyme AlgE6 or the bifunctional AlgE7 it is apparent that only subtle differences result in very different activities. Now that the structure of AlgE4 is known, it is possible to form and test hypotheses as to which amino acids are responsible for the various properties. The answers to these questions will also create a deeper understanding of the reaction mechanism of these enzymes. Given the striking similarities of the active sites of the studied epimerases and lyases, the results presented here may also help in understanding substrate binding, and hence the substrate specificities of the different enzymes involved in alginate cleavage or epimerization.

Acknowledgments—We thank Drs. A Coetzee and B. Schierbeek for collection of the M_4 data at Bruker-AXS and T. Pijning for critical reading of the manuscript.

REFERENCES

1. Fischer, F. G., and Dörfel, H. (1955) *Hoppe-Seyler's Z. Physiol. Chem.* **302,** 186–203
2. Drummond, D. W., Hirst, E. L., and Percival, E. (1962) *J. Chem. Soc.* pp. 1208–1216
3. Linker, A., and Jones, R. S. (1964) *Nature* **204,** 187–188
4. Gorin, P. A. J., and Spencer, J. F. T. (1966) *Can. J. Chem.* **44,** 993–998
5. Donati, I., Holtan, S., Mørch, Y. A., Borgogna, M., Dentini, M., and Skjåk-Bræk, G. (2005) *Biomacromolecules* **6,** 1031–1040

6. Lin, L. P., and Sadoff, H. L. (1969) *J. Bacteriol.* **100,** 480–486
7. Sadoff, H. L. (1975) *Bacteriol. Rev.* **39,** 516–539
8. Campos, M. E., Martínez-Salazar, J. M., Lloret, L., Moreno, S., Núñez, C., Espín, G., and Soberón-Chávez, G. (1996) *J. Bacteriol.* **178,** 1793–1799
9. Sabra, W., Zeng, A. P., Lünsdorf, H., and Deckwer, W. D. (2000) *Appl. Env. Microbiol.* **66,** 4037–4044
10. Valla, S., Li, J. P., Ertesvåg, H., Barbeyron, T., and Lindahl, U. (2001) *Biochimie* (*Paris*) **83,** 819–830
11. Rehm, B. H., Ertesvåg, H., and Valla, S. (1996) *J. Bacteriol.* **178,** 5884–5889
12. Ertesvåg, H., Høidal, H. K., Hals, I. K., Rian, A., Doseth, B., and Valla, S. (1995) *Mol. Microbiol.* **16,** 719–731
13. Svanem, B. I. G., Skjåk-Bræk, G., Ertesvåg, H., and Valla, S. (1999) *J. Bacteriol.* **181,** 68–77
14. Ertesvåg, H., and Valla, S. (1999) *J. Bacteriol.* **181,** 3033–3038
15. Ramstad, M. V., Ellingsen, T. E., Josefsen, K. D., Høidal, H. K., Valla, S., Skjåk-Bræk, G., and Levine, D. W. (1999) *Enzyme Microb. Technol.* **24,** 636–646
16. Høidal, H., Ertesvåg, H., Skjåk-Bræk, G., Stokke, B. T., and Valla, S. (1999) *J. Biol. Chem.* **274,** 12316–13322
17. Sletmoen, M., Skjåk-Bræk, G., and Stokke, B. T. (2004) *Biomacromolecules* **5,** 1288–1295
18. Aachmann, F. L., Svanem, B. I. G., Güntert, P., Petersen, S. B., Valla, S., and Wimmer, R. (2006) *J. Biol. Chem.* **281,** 7350–7356
19. Campa, C., Holtan, S., Nilsen, N., Bjerkan, T. M., Stokke, B. T., and Skjåk-Bræk, G. (2004) *Biochem. J.* **381,** 155–164
20. Hartmann, M., Holm, O. B., Johansen, G. A. B., Skjåk-Bræk, G., and Stokke, B. T. (2002) *Biopolymers* **63,** 77–88
21. Svanem, B. I. G., Strand, W. I., Ertesvåg, H., Skjåk-Bræk, G., Hartmann, M., Barbeyron, T., and Valla, S. (2001) *J. Biol. Chem.* **276,** 31542–31550
22. Nyvall, P., Corre, E., Boisset, C., Barbeyron, T., Rousvoal, S., Scornet, D., Kloareg, B., and Boyen, C. (2003) *Plant Physiol.* **133,** 726–735
23. Douthit, S. A., Dlakic, M., Ohman, D. E., and Franklin, M. J. (2005) *Bacteriol. J.* **187,** 4573–4583
24. Gacesa, P. (1987) *FEBS Lett.* **212,** 199–202
25. Sambrook, J., and Russell, D. (2001) *Molecular Cloning: A Laboratory Manual*, Third Ed., Cold Spring Harbor Laboratory Press, Cold Spring Harbor, NY
26. Andrade, M. A., Chacón, P., Merelo, J. J., and Morán, F. (1993) *Protein Eng.* **6,** 383–390
27. McPherson, A. (2001) *Protein Sci.* **10,** 418–422
28. Otwinowski, Z., and Minor, W. (1997) *Methods Enzymol.* **276,** 307–326
29. Matthews, B. W. (1968) *J. Mol. Biol.* **33,** 491–497
30. Bluhm, M. M., Bodo, G., Dintzis, H. M., and Kendrew, J. C. (1958) *Proc. R. Soc. A* **246,** 369–389
31. Terwilliger, T. C. (2003) *Methods Enzymol.* **374,** 22–37
32. Jones, T. A., Zou, J. Y., Cowan, S. W., and Kjeldgaard, M. (1991) *Acta Crystallogr. Sect. A* **47,** 110–119
33. Morris, R. J., Perrakis, A., and Lamzin, V. S. (2003) *Methods Enzymol.* **374,** 229–244
34. Brünger, A. T., Adams, P. D., Clore, G. M., DeLano, W. L., Gros, P., Grosse-Kunstleve, R. W., Jiang, J. S., Kuszewski, J., Nilges, M., Pannu, N. S., Read, R. J., Rice, L. M., Simonson, T., and Warren, G. L. (1998) *Acta Crystallogr. Sect. D Biol. Crystallogr.* **54,** 905–921
35. Laskowski, R. A., MacArthur, M. W., Moss, D. S., and Thornton, J. M. (1993) *J. Appl. Crystallogr.* **26,** 283–291
36. Bradford, M. M. (1976) *Anal. Biochem.* **72,** 248–254
37. van Santen, Y., Benen, J. A. E., Schröter, K. H., Kalk, K. H., Armand, S., Visser, J., and Dijkstra, B. W. (1999) *J. Biol. Chem.* **274,** 30474–30480
38. Kabsch, W., and Sander, C. (1983) *Biopolymers* **22,** 2577–2637
39. Jenkins, J., Shevchik, V. E., Hugouvieux-Cotte-Pattat, N., and Pickersgill, R. W. (2004) *J. Biol. Chem.* **279,** 9139–9145
40. van Pouderoyen, G., Snijder, H. J., Benen, J. A. E., and Dijkstra, B. W. (2003) *FEBS Lett.* **554,** 462–466
41. Jabs, A., Weiss, M. S., and Hilgenfeld, R. (1999) *J. Mol. Biol.* **286,** 291–304
42. Yoon, H. J., Hashimoto, W., Miyake, O., Murata, K., and Mikami, B. (2001) *J. Mol. Biol.* **307,** 9–16
43. Holm, L., and Sander, C. (1993) *J. Mol. Biol.* **233,** 123–138
44. Coutinho, P. M., and Henrissat, B. (1999) in *Recent Advances in Carbohydrate Bioengineering* (Gilbert, H. J., Davies, G., Henrissat, B., and Svensson, B., eds) pp. 3–12, The Royal Society of Chemistry, Cambridge
45. Yoon, H. J., Mikami, B., Hashimoto, W., and Murata, K. (1999) *J. Mol. Biol.* **290,** 505–514
46. Yamasaki, M., Moriwaki, S., Miyake, O., Hashimoto, W., Murata, K., and Mikami, B. (2004) *J. Biol. Chem.* **279,** 31863–31872
47. Osawa, T., Matsubara, Y., Muramatsu, T., Kimura, M., and Kakuta, Y. (2005) *J. Mol. Biol.* **345,** 1111–1118
48. Yamasaki, M., Ogura, K., Hashimoto, W., Mikami, B., and Murata, K. (2005) *J. Mol. Biol.* **352,** 11–21
49. Huang, W. J., Boju, L., Tkalec, L., Su, H. S., Yang, H. O., Gunay, N. S., Linhardt, R. J., Kim, Y. S., Matte, A., and Cygler, M. (2001) *Biochemistry* **40,** 2359–2372
50. Rye, C. S., Matte, A., Cygler, M., and Withers, S. G. (2006) *ChemBioChem* **7,** 631–637
51. Bjerkan, T. M., Lillehov, B. E., Strand, W. I., Skjåk-Bræk, G., Valla, S., and Ertesvåg, H. (2004) *Biochem. J.* **381,** 813–821
52. DeLano, W. L. (2002) *The PyMOL Molecular Graphics System,* DeLano Scientific, Palo Alto, CA
53. Blatny, J. M., Brautaset, T., Winther-Larsen, H. C., Karunakaran, P., and Valla, S. (1997) *Plasmid* **38,** 35–51